

Published in final edited form as:

Arch Ophthalmol. 2012 March ; 130(3): 343–349. doi:10.1001/archophthalmol.2011.381.

Extraocular Muscles in Patients With Infantile Nystagmus:

Adaptations at the Effector Level

Kathleen T. Berg, BS, David G. Hunter, MD, PhD, Erick D. Bothun, MD, Rosalia Antunes-Foschini, MD, and Linda K. McLoon, PhD

Departments of Ophthalmology (Ms Berg and Drs Bothun and McLoon), Pediatrics (Dr Bothun), and Neuroscience (Dr McLoon), University of Minnesota, Minneapolis; Department of Ophthalmology, Children's Hospital Boston, Harvard Medical School, Boston, Massachusetts (Dr Hunter); and Department of Ophthalmology, Faculty of Medicine of Ribeirao Preto, University of São Paulo, São Paulo, Brazil (Dr Antunes-Foschini)

Abstract

Objective—To test the hypothesis that the extraocular muscles (EOMs) of patients with infantile nystagmus have muscular and innervational adaptations that may have a role in the involuntary oscillations of the eyes.

Methods—Specimens of EOMs from 10 patients with infantile nystagmus and postmortem specimens from 10 control subjects were prepared for histologic examination. The following variables were quantified: mean myofiber cross-sectional area, myofiber central nucleation, myelinated nerve density, nerve fiber density, and neuromuscular junction density.

Results—In contrast to control EOMs, infantile nystagmus EOMs had significantly more centrally nucleated myofibers, consistent with cycles of degeneration and regeneration. The EOMs of patients with nystagmus also had a greater degree of heterogeneity in myofiber size than did those of controls, with no difference in mean myofiber cross-sectional area. Mean myelinated nerve density, nerve fiber density, and neuromuscular junction density were also significantly decreased in infantile nystagmus EOMs.

Conclusions—The EOMs of patients with infantile nystagmus displayed a distinct hypoinnervated phenotype. This represents the first quantification of changes in central nucleation and myofiber size heterogeneity, as well as decreased myelinated nerve, nerve fiber, and neuromuscular junction density. These results suggest that deficits in motor innervation are a potential basis for the primary loss of motor control.

Clinical Relevance—Improved understanding of the etiology of nystagmus may direct future diagnostic and treatment strategies.

Infantile nystagmus syndrome is an eye movement disorder characterized by uncontrolled bilateral oscillatory eye movements, with a prevalence of approximately 2 per 1000 people.^{1,2} The oscillatory movements associated with infantile nystagmus syndrome are usually horizontal and conjugate, with characteristic jerk or pendular waveforms.³ The cause of infantile nystagmus syndrome is poorly understood. Often, nystagmus is associated with reduced visual acuity occurring early in life secondary to structural abnormalities in the afferent visual pathways.³ In these cases, the nystagmus may be due to abnormal

©2012 American Medical Association. All rights reserved.

Correspondence: Linda K. McLoon, PhD, Department of Ophthalmology, University of Minnesota, 2001 Sixth St SE, Room 374 Lions Research Bldg, Minneapolis, MN 55455 (mcloo001@umn.edu).

Financial Disclosure: None reported.

development of 1 or more areas of the brain that control eye movements and gaze stability.⁴ Even less is understood about the cause of infantile nystagmus occurring in the absence of such sensory deficits. The genetic association of some forms of nystagmus with mutations in proteins known to cause changes in nerve growth patterns⁵ suggests that infantile nystagmus may be caused by a dysregulation of innervation. This observation supports the hypothesis that infantile nystagmus may be due to hypoinnervation, misrouting of the nerves that innervate the extraocular muscles (EOMs), or both. Hypoinnervation in this context is defined as a decreased density of nerves based on the mean muscle cross-sectional area or mean myofiber number. Hypoinnervation, with the accompanying reduced neuromuscular junction density, would, in turn, lead to a decrease in myofiber size, myofiber number, or both in the EOMs of these patients. Nystagmus might then be a result of the inability of the brain to compensate for insufficient functional muscle or insufficient adaptability in the residual EOMs to allow the normal exquisite control over eye position and eye movements.

This study tested the hypothesis that the EOMs in patients with infantile nystagmus would display a decrease in myofiber size and a decrease in overall motor nerve density, demonstrated by decreases in total myelinated nerve, nerve fiber, and neuromuscular junction density. Discarded EOMs were obtained from patients with infantile nystagmus without known sensory deficits after standard surgical resection procedures for the treatment of their disorder. These EOMs were compared with control EOMs of the same approximate distal tendon length obtained during eye bank removal of eyes or as cadaveric material.

METHODS

All control material was obtained with informed consent for research use from either cadaveric material or during University of Minnesota Eye Bank harvesting of human eyes. Five medial rectus, 3 superior rectus, and 2 inferior oblique muscles were obtained from control muscle donors aged 7 to 74 years, with a mean (SD) age of 34.8 (6.6) years. All tissue was kept on ice or refrigerated until frozen. The interval from time of death to muscle harvesting ranged from 4.5 to 24 hours, with a mean of 7 hours. Only 10 control muscles, those that showed no histologic evidence of postmortem degeneration, were included. The 10 control muscles selected for this analysis were all histologically normal in appearance. Specifically, normal sarcomeric integrity was evident in the control samples analyzed for this study, and the muscles showed no evidence of sarcolemmal dissolution, loss of nuclear staining, or kinking.⁶ Two muscles (medial rectus and inferior oblique) obtained from a 7-year-old child whose death was not related to head trauma were also included in the control group. These 2 child muscles were fixed in 10% formalin and paraffin embedded. This treatment results in shrinkage of approximately 10%, which was calculated into the measurements made on this tissue.⁷ An additional muscle was obtained as surgical waste from a 4½-year-old child diagnosed as having hypertropia at the time of resection surgery. Only the distal 6 to 10 mm from all control and patient muscles were analyzed to ensure that similar regions of control and patient muscles were compared.

The EOM specimens from patients with infantile nystagmus were obtained as discarded surgical material from scheduled surgery for patients being treated at either the University of Minnesota or Children's Hospital Boston. Patients with previous EOM surgery were excluded. In addition, none of the patients had known sensory defects. Patient age, diagnosis, clinical synopsis with all personally identifiable health information removed, and muscle identification were transmitted along with the specimen. All the patient EOMs, except the noted exception, were embedded in tragacanth gum and frozen in methylbutane chilled to a slurry on liquid nitrogen. This research received institutional review board approval from the University of Minnesota and Children's Hospital Boston and adhered to the Declaration of Helsinki for the use of human tissue in research. All the work was Health

Insurance Portability and Accountability Act compliant. The primary diagnosis of each patient, patient age at the time of surgery, and muscles resected are listed in the Table. The mean (SD) age of the patients was 11.1 (4.6) years, with an age range of 4 to 52 years. In some cases, analysis of the young donor muscle was presented separately. Although it could not be used for statistical purposes, the separate analysis performed was important to demonstrate potential alterations that might be age specific.

One normal juvenile monkey medial rectus muscle was also obtained at the time of animal euthanasia from another investigator (with Institutional Animal Care and Use Committee approval), frozen, and processed for immunohistochemical visualization of neuromuscular junctions. This procedure was performed to obtain a muscle that more closely resembled the chronological age of the human child infantile nystagmus muscle and whose length was not altered by fixatives. Connective tissue density changes in EOMs with age, and this could also affect the calculated density of neuromuscular junctions.

Ten infantile nystagmus EOMs (Table) and 10 control EOMs were examined. The muscles were sectioned longitudinally at 12 μm , air-dried onto slides, and processed for histologic and morphometric examination. Because all the muscles had sections that were in both longitudinal and cross-sectional orientations, it was also possible to analyze cross-sectional material. Tissue sections were processed using several methods. Hematoxylin-eosin-stained EOMs were used to determine the percentage of myofibers in cross section with central nucleation. Myofiber cross-sectional areas were measured, and the mean cross-sectional area for each population was calculated. A histogram of myofiber area measurements in patients and controls was created in 100- μm increments.

Additional sections were immunostained for Schwann cell myelin (1:50) (Cosmo Bio Co Ltd) or neurofilament protein (1:1000) (Covance), followed by incubation using the Vectastain Elite ABC Kit (Vector Laboratories) and reacted using the diaminobenzidine procedure with heavy metal intensification. Sections were analyzed for area positive for Schwann cell myelin or nerve fibers as a percentage of total muscle area per cross section examined.

For neuromuscular junction density measurements, longitudinal sections were immunostained using an antibody to the α -1, α -3, and α -5 subunits of the nicotinic acetylcholine receptor (1:500) (Sigma-Aldrich Corp) conjugated to Alexa Fluor 488 (1:200) (Invitrogen). The neuromuscular junctions were quantified using image analysis software (Topographer program of Bioquant NovaPrime; Bioquant) using a video camera mounted to a microscope (Leica DMR; Leica Microsystems).⁸ First, the entire cross-sectional area of the muscle in longitudinal section was determined at $\times 1.5$ magnification. This was followed by visualization at $\times 20$ magnification and recording of each neuromuscular junction that was located. Approximately every 10th slide that contained longitudinal sections of muscle was analyzed. The Bioquant Topographer program records the x and y coordinates and can reconstruct the area outlines and neuromuscular junction locations and determine junctional density, calculated as the number of neuromuscular junctions per square millimeter.

For statistical purposes, the adult control and child control data were pooled. The mean cross-sectional areas, percentage central nucleation results, and neuromuscular density comparisons were analyzed using the unpaired t test, with the Welch correction for unequal variances, using the Prism and Stat-Mate programs (GraphPad Software, Inc). A statistical comparison was performed between both distributions of the binned myofiber cross-sectional areas using the Levene test for equality of variances. Data were considered statistically significantly different at $P < .05$.

RESULTS

The EOM mean myofiber cross-sectional area was not significantly different in patients with infantile nystagmus compared with in controls, including adult and child muscles (Figure 1 and Figure 2). However, myofiber heterogeneity was increased in muscles from patients with infantile nystagmus when single muscles were compared (Figure 3A) and when the muscles were pooled (Figure 3B). The primary source of heterogeneity was the increase in numbers of very small and very large myofibers in muscles from patients with infantile nystagmus (Figure 3A). The variances between the 2 populations were significantly different ($P < .001$).

Central nucleation is usually seen in patients whose muscles are undergoing cycles of degeneration and regeneration. Mean (SE) levels of central nucleation were elevated 10-fold in infantile nystagmus muscles (23.77% [1.99%] of myofibers) compared with in control muscles (1.9% [0.34%] of myofibers; and 0.42% [0.2%] of myofibers in the child muscle) (Figure 4).

Based on the elevated numbers of myofibers with central nucleation, nerve density was assessed using an antibody to Schwann cell myelin. Examination of immunostained tissue sections suggested that there was a decreased density of myelinated nerves in infantile nystagmus muscles compared with control muscles (Figure 5A and B). The specificity of this effect is magnified compared with the myelinated nerve content in a muscle from a patient with vertical strabismus (Figure 5C).⁹ When quantified as a percentage of total muscle area, mean (SE) myelinated nerve density was reduced 10-fold in muscles from patients with infantile nystagmus ($0.10/\mu\text{m}^2$ [$0.01/\mu\text{m}^2$]) compared with those from controls ($1.13/\mu\text{m}^2$ [$0.1/\mu\text{m}^2$]) (Figure 5D).

To confirm that the density changes were not due to loss of myelination, the density of nerve fibers per muscle area was assessed using sections immunostained for neurofilament protein. Mean (SE) nerve fiber density in control muscles was $1.69/\mu\text{m}^2$ ($0.21/\mu\text{m}^2$) compared with $0.31/\mu\text{m}^2$ ($0.06/\mu\text{m}^2$) in muscles from patients with infantile nystagmus, more than a 5-fold reduction (Figure 6).

The hypoinnervated phenotype was confirmed further using immunostaining for visualization of neuromuscular junctions, which were quantified in longitudinal muscle sections (Figure 7). Three-dimensional reconstructions showed the relative paucity of neuromuscular junctions in infantile nystagmus EOMs compared with the distal one-third of a normal monkey EOM (Figure 7A and B). The mean (SE) neuromuscular junction density in muscles from patients with infantile nystagmus was reduced 6-fold (1.1 [0.45] junctions/ mm^2) compared with that in muscles from controls (6.9 [1.13] junctions/ mm^2) (Figure 7C).

In the surgical control specimen from the child with vertical strabismus, myofiber heterogeneity and central nucleation were similar to those observed in postmortem controls (data not shown), whereas nerve density was significantly elevated compared with that of control muscles (Figure 5C). These findings support the view that surgical specimens from patients with different diagnoses have distinct phenotypes, and these can also be distinct from those of control EOM samples.

COMMENT

In this study, EOMs removed during corrective surgery for infantile nystagmus were compared with control EOMs removed 4.5 to 24 hours postmortem. We are confident that the differences observed are not secondary to postmortem artifact for several reasons. First, in muscles that show other histologic evidence of postmortem degeneration, to our

knowledge, there is no published evidence that demonstrates changes in myofiber heterogeneity, central nucleation, or density of myelinated nerves, neurofilament-positive axons, and neuromuscular junctions.^{10,11} As these are all active processes, it would be unlikely that these types of changes would occur artifactually. Second, the present data include a nystagmus specimen obtained from a 52-year-old that demonstrated the same phenotype as the nystagmus specimens from children and was notably different from the EOMs of controls. Third, the muscle resection specimen obtained intraoperatively from a young child without nystagmus had values for most of the previously mentioned variables that were within the range of values observed in controls.

Although infantile nystagmus is often considered idiopathic, it can be associated with afferent sensory defects, including optic nerve hypoplasia, albinism, retinal dystrophies, aniridia, and Leber congenital amaurosis.^{12,13} As indicated in the Table, all the infantile nystagmus patients in the present study were considered “idiopathic” and their nystagmus unrelated to known afferent sensory abnormalities. Ongoing studies will determine whether the same phenotype is seen in muscles from patients with infantile nystagmus with abnormal sensory components.

All infantile nystagmus muscles examined displayed the same phenotype: increased myofiber cross-sectional area heterogeneity, increased central nucleation, decreased overall myelinated nerve density and nerve fiber density, and concomitant decreased neuromuscular junction density compared with postmortem and surgical controls. These findings support the working hypothesis that infantile nystagmus syndrome is associated with hypoinnervation compared with normal EOM. This observation suggests that these differences would most likely result in increased motor unit size, although this was not testable in the patient muscles.

Mammalian EOMs, including human EOMs, are known to undergo continuous remodeling in normal adults.¹⁴⁻¹⁶ However, this process normally maintains the typical pattern of peripheral nucleation of adult EOM myofibers. Central nucleation has long been associated with muscle disease and muscle injury and regeneration.^{17,18} Based on the increased percentage of centrally nucleated myofibers, the EOMs from these patients seem to be undergoing more rapid cycles of degeneration and regeneration than are those of controls. Although a dynamic process cannot be assessed from histologic specimens, the presence of central nucleation was a consistent finding in the patients’ muscles, suggesting that this indeed may be the case. The cause of this process is unknown. There is little documentation of percentage changes in centrally nucleated myofibers in normal aging skeletal muscle, although its incidence increases in diseased aging muscle.¹⁹ Thus, control EOMs would potentially overrepresent the number of centrally nucleated myofibers in healthy EOMs, therefore underrepresenting the true difference between patient and control EOMs. This finding is supported further by the scarcity of centrally nucleated myofibers in the muscle from the 7-year-old control. It may also be possible that congenitally decreased innervational density may result in delayed or arrested development. Future laboratory experiments are needed to test this hypothesis.

The *FRMD7* gene associated with infantile nystagmus is known to affect axon outgrowth during development.²⁰ Thus, the results of the present study are aligned with known sequelae of the effects of abnormal axonal development. Because genetic testing is not currently part of the normal medical care of patients with infantile nystagmus, the presence of *FRMD7* gene mutations is unknown in the present population. Despite their unknown genetic status, it is possible that some of the patients had mutations in the *FRMD7* gene; in a Chinese cohort of patients with infantile nystagmus, 47% had a mutation in the *FRMD7* gene locus.²¹ It is unclear from these specimens whether the changes in the EOMs are

secondary to innervational problems in development. The *FRMD7* studies support the hypothesis that other forms of infantile nystagmus syndrome are also likely to have nerve maldevelopment as their primary cause. Future genetic studies are needed to clarify this issue.

Several studies^{22,23} have examined EOMs from patients with ocular motility disorders, including EOMs from patients diagnosed as having infantile nystagmus, but these studies focused on EOM ultrastructure and pathologic characteristics at the single-fiber level. Several abnormalities were described in these studies, including myofibrillar disruption and abnormal mitochondria. Similar changes were described in EOMs from patients with strabismus, but the same features also were seen in control EOMs.²⁴ Thus, care must always be taken when interpreting electron micrographs from EOMs as they have many histologic characteristics distinct from other skeletal muscles.²⁵ The present analysis focused on changes that were quantifiable and clearly visible using standard light microscopy. Changes in innervation, fiber size heterogeneity, and central nucleation were seen in all the surgically resected EOMs from the 10 patients with infantile nystagmus. We are continuing to collect and analyze muscle specimens from patients with infantile nystagmus and other ocular motility disorders. Future studies, which will include examination of genetic mutations, may allow more accurate determination of nystagmus subtypes.

In conclusion, all the EOMs from patients with infantile nystagmus displayed similar histologic alterations, including increased myofiber cross-sectional area heterogeneity, increased central nucleation, hypoinnervation, and reduced neuromuscular junction density. These results support the hypothesis that deficits in motor innervation may be a primary cause of the inability of the oculomotor system to control eye position and movements in infantile nystagmus. An improved understanding of the pathogenesis of infantile nystagmus should permit the exploration of more targeted treatment methods in the future.

Acknowledgments

Funding/Support: This study was supported by grants EY15313 and EY11375 from the National Eye Institute, the Minnesota Medical Foundation, Minnesota Lions and Lionesses, a Fight for Sight Medical Student Fellowship (Ms Berg), Children's Hospital Ophthalmology Foundation, Boston, Massachusetts; and an unrestricted grant to the Department of Ophthalmology, University of Minnesota, from Research to Prevent Blindness.

References

1. Sarvananthan N, Surendran M, Roberts EO, et al. The prevalence of nystagmus: the Leicestershire nystagmus survey. *Invest Ophthalmol Vis Sci.* 2009; 50(11):5201–5206. [PubMed: 19458336]
2. Stayte M, Reeves B, Wortham C. Ocular and vision defects in preschool children. *Br J Ophthalmol.* 1993; 77(4):228–232. [PubMed: 8494859]
3. Abadi RV, Bjerre A. Motor and sensory characteristics of infantile nystagmus. *Br J Ophthalmol.* 2002; 86(10):1152–1160. [PubMed: 12234898]
4. Jacobs JB, Dell'Osso LF. Congenital nystagmus: hypotheses for its genesis and complex waveforms within a behavioral ocular motor system model. *J Vis.* 2004; 4(7):604–625. [PubMed: 15330705]
5. Tarpey P, Thomas S, Sarvananthan N, et al. Mutations in *FRMD7*, a newly identified member of the FERM family, cause X-linked idiopathic congenital nystagmus. *Nat Genet.* 2006; 38(11):1242–1244. published correction appeared in *Nat Genet.* 2011; 43(7):720. [PubMed: 17013395]
6. MacNaughtan AF. A histological study of post mortem changes in the skeletal muscle of the fowl (*Gallus domesticus*), I: the muscle fibres. *J Anat.* 1978; 125(pt 3):461–476. [PubMed: 640953]
7. Boonstra H, Oosterhuis JW, Oosterhuis AM, Fleuren GJ. Cervical tissue shrinkage by formaldehyde fixation, paraffin wax embedding, section cutting and mounting. *Virchows Arch A Pathol Anat Histopathol.* 1983; 402(2):195–201. [PubMed: 6420986]

8. Harrison AR, Anderson BC, Thompson LV, McLoon LK. Myofiber length and three-dimensional localization of NMJs in normal and botulinum toxin treated adult extraocular muscles. *Invest Ophthalmol Vis Sci.* 2007; 48(8):3594–3601. [PubMed: 17652728]
9. McLoon LK, Kohl J, Stager D Jr. Innervation changes in inferior oblique muscles from patients with over-elevation in adduction. *Invest Ophthalmol Vis Sci.* 2011; 52:2078. ARVO abstract.
10. Goldspink G, Gelder S, Clapison L, Overfield P. Pre- and post-rigor fixation of muscle. *J Anat.* 1973; 114(pt 1):1–6. [PubMed: 4577028]
11. MacNaughtan AF. A histological study of post mortem changes in the skeletal muscle of the fowl (*Gallus domesticus*), II: the cytoarchitecture. *J Anat.* 1978; 126(pt 1):7–20. [PubMed: 649504]
12. Casteels I, Harris CM, Shawkat F, Taylor D. Nystagmus in infancy. *Br J Ophthalmol.* 1992; 76(7):434–437. [PubMed: 1627515]
13. Gottlob I. Nystagmus. *Curr Opin Ophthalmol.* 2000; 11(5):330–335. [PubMed: 11148698]
14. McLoon LK, Rowe J, Wirtschafter J, McCormick KM. Continuous myofiber remodeling in uninjured extraocular myofibers: myonuclear turnover and evidence for apoptosis. *Muscle Nerve.* 2004; 29(5):707–715. [PubMed: 15116375]
15. McLoon LK, Wirtschafter JD. Continuous myonuclear addition to single extraocular myofibers in uninjured adult rabbits. *Muscle Nerve.* 2002; 25(3):348–358. [PubMed: 11870711]
16. McLoon LK, Wirtschafter J. Activated satellite cells in extraocular muscles of normal adult monkeys and humans. *Invest Ophthalmol Vis Sci.* 2003; 44(5):1927–1932. [PubMed: 12714625]
17. Grounds MD, McGeachie JK. Myogenic cell replication in minced skeletal muscle isografts of Swiss and BALBc mice. *Muscle Nerve.* 1990; 13(4):305–313. [PubMed: 2355943]
18. Pisani V, Panico MB, Terracciano C, et al. Preferential central nucleation of type 2 myofibers is an invariable feature of myotonic dystrophy type 2. *Muscle Nerve.* 2008; 38(5):1405–1411. [PubMed: 18816606]
19. Marques MJ, Ferretti R, Vomero VU, Minatel E, Neto HS. Intrinsic laryngeal muscles are spared from myonecrosis in the mdx mouse model of Duchenne muscular dystrophy. *Muscle Nerve.* 2007; 35(3):349–353. [PubMed: 17143878]
20. Betts-Henderson J, Bartesaghi S, Crosier M, et al. The nystagmus-associated *FRMD7* gene regulates neuronal outgrowth and development. *Hum Mol Genet.* 2010; 19(2):342–351. [PubMed: 19892780]
21. He X, Gu F, Wang Z, et al. A novel frameshift mutation in *FRMD7* causing X-linked idiopathic congenital nystagmus. *Genet Test.* 2008; 12(4):607–613. [PubMed: 19072571]
22. Mencucci R, Domenici-Lombardo L, Cortesini L, Faussonne-Pellegrini MS, Salvi G. Congenital nystagmus: fine structure of human extraocular muscles. *Ophthalmologica.* 1995; 209(1):1–6. [PubMed: 7715919]
23. Peng GH, Zhang C, Yang JC. Ultrastructural study of extraocular muscle in congenital nystagmus. *Ophthalmologica.* 1998; 212(1):1–4. [PubMed: 9438576]
24. Berard-Badier M, Pellissier JF, Toga M, Mouillac N, Berard PV. Ultrastructural studies of extraocular muscles in ocular motility disorders, II: morphological analysis of 38 biopsies. *Albrecht Von Graefes Arch Klin Exp Ophthalmol.* 1978; 208(1-3):193–205. [PubMed: 215049]
25. McLoon, LK. The extraocular muscles. In: Kaufman, P.; Alm, A.; Levin, LA.; Nilsson, S.; Ver Hoeve, J.; Wu, SM., editors. *Adler's Physiology of the Eye.* 11. St Louis, MO: Mosby Press; 2011. p. 182-207.

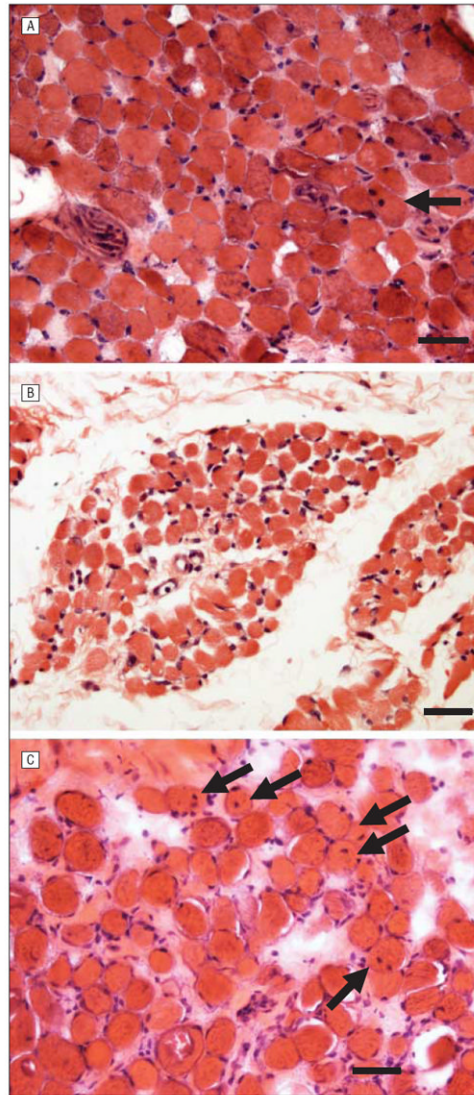


Figure 1. Light microscopic examination of control and patient extraocular muscles stained with hematoxylin-eosin. Comparison of hematoxylin-eosin stains of muscles from adult controls (A), the child control (paraffin embedded) (B), and patients with infantile nystagmus (C). Arrows indicate myofibers with centrally located myonuclei. Bar is 20 μm .

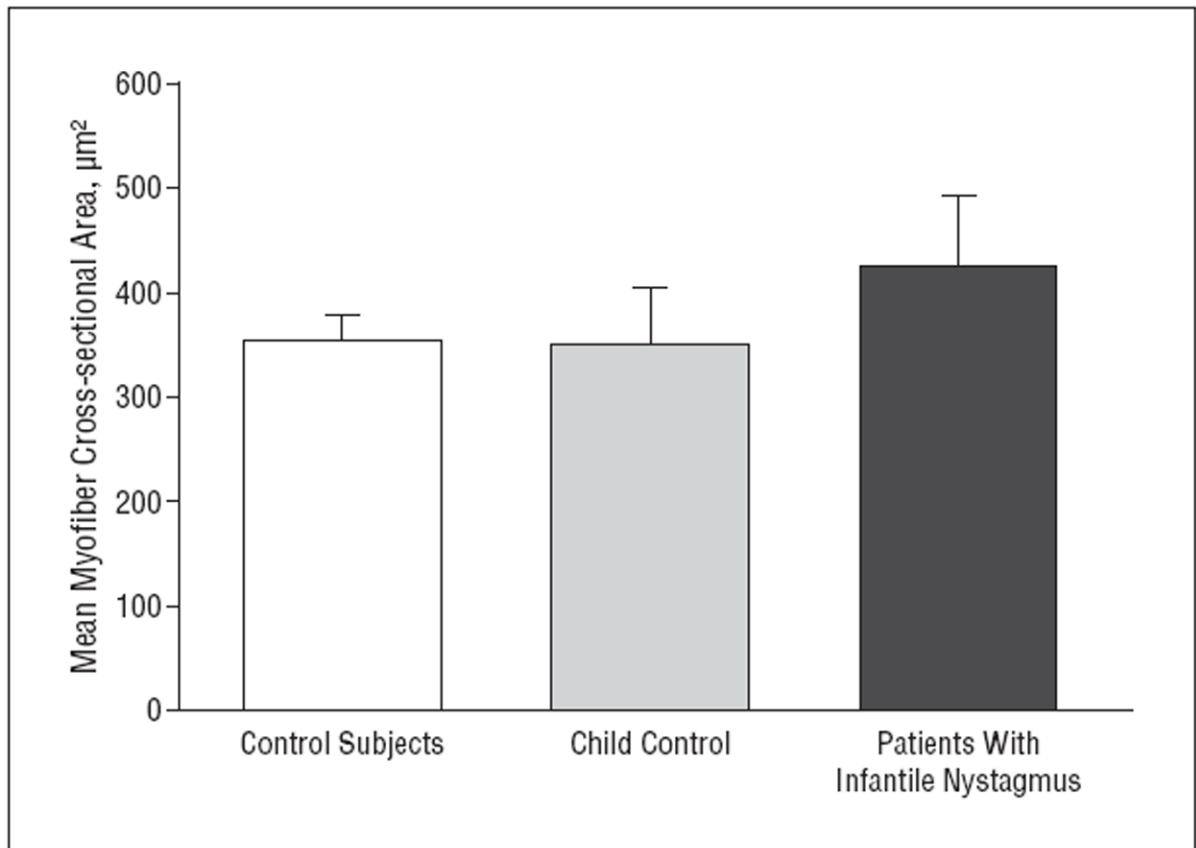


Figure 2.

Quantification of the mean myofiber cross-sectional area in normal rectus muscles compared with all the muscles from patients with infantile nystagmus. The mean values are not statistically significantly different. Mean myofiber area for the child control muscle is displayed separately for comparative purposes. Because there were only 2 such muscles, both from 1 donor, no comparative statistics were performed. However, the mean values overlap, strongly suggesting that there is no difference between the aggregated control muscles and the control muscles from the child donor. Error bars represent SE.

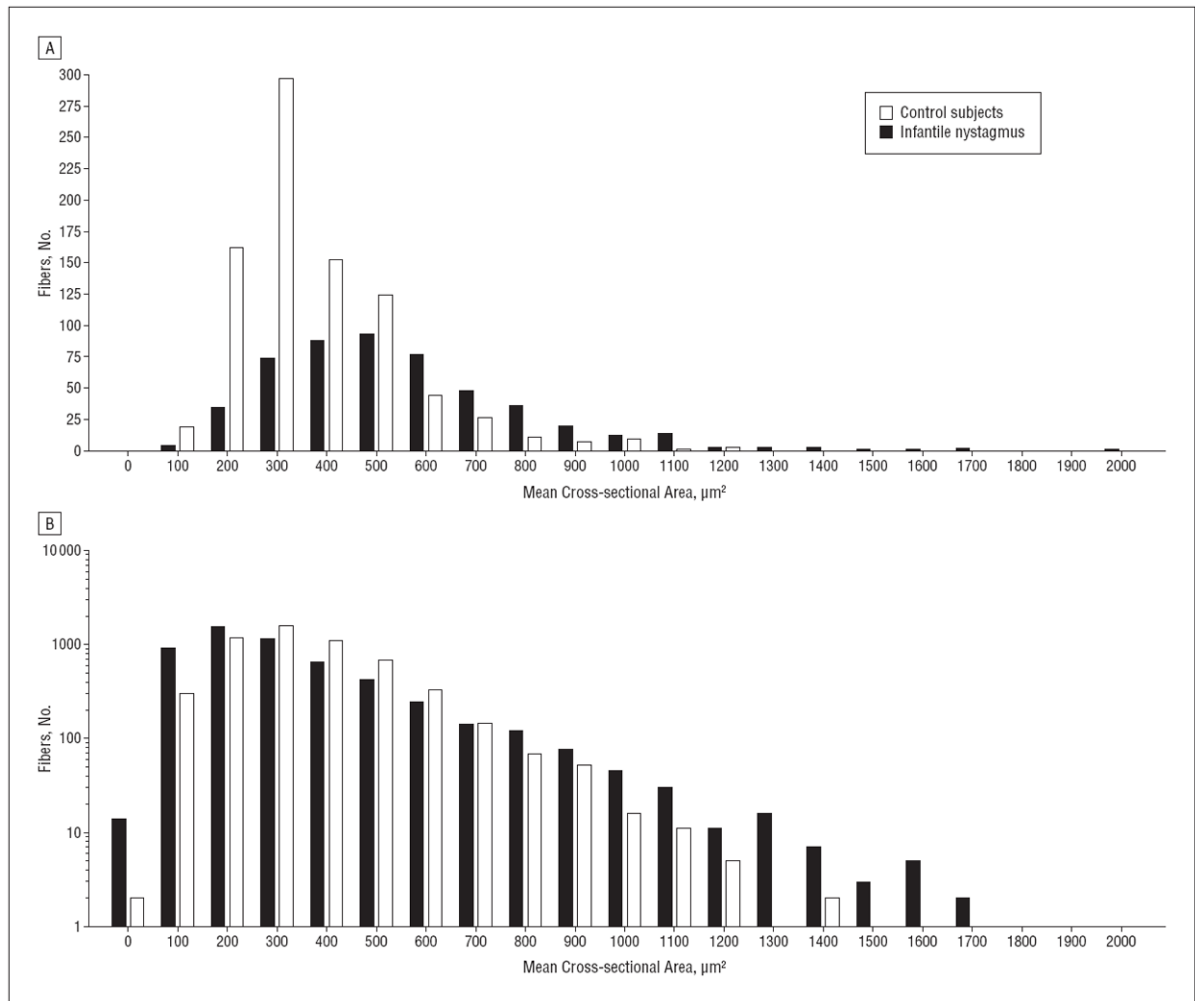


Figure 3. Histograms of myofiber size demonstrating increased heterogeneity of myofiber cross-sectional areas in muscles from patients with infantile nystagmus. A, Histogram of myofiber cross-sectional areas from medial rectus muscles from 1 control (case 2) and 1 patient with infantile nystagmus (patient 5). The y-axis is in \log_{10} . B, Histogram of aggregated myofiber cross-sectional areas from extraocular muscles from controls and patients with infantile nystagmus. The y-axis is in \log_{10} .

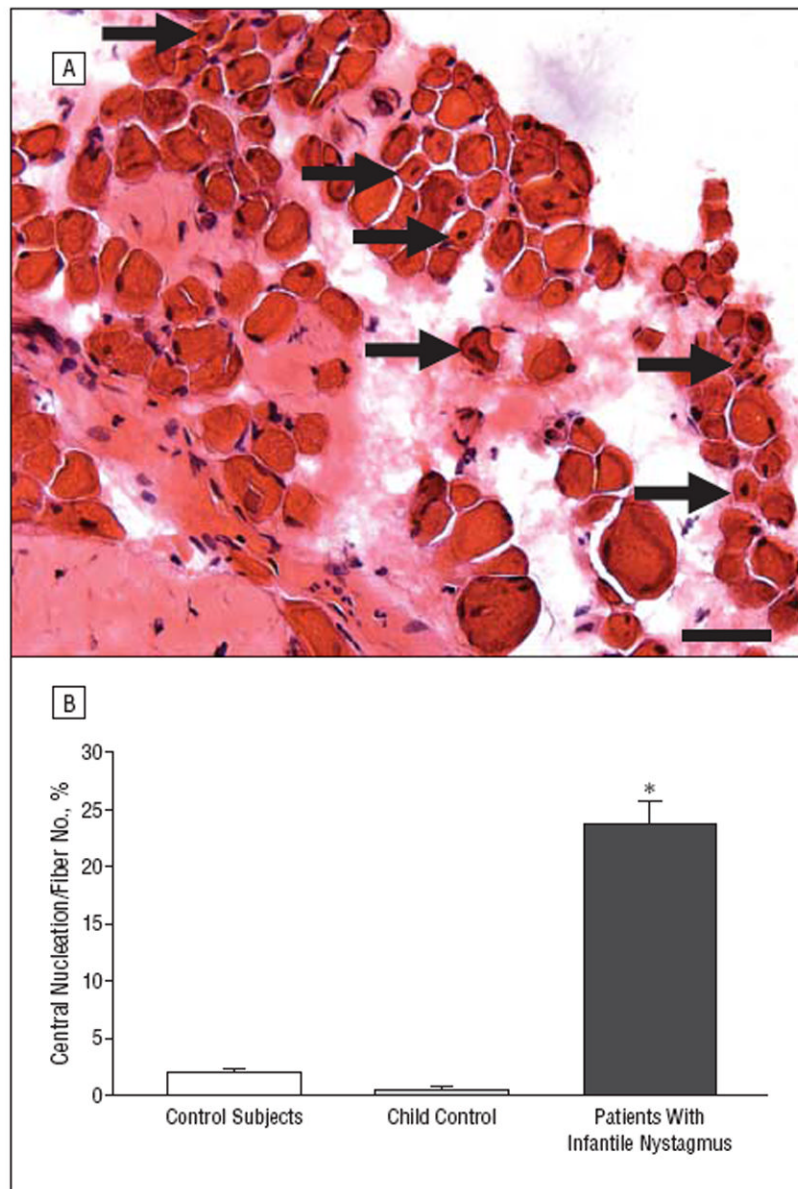


Figure 4. Central nucleation in controls and in patients with infantile nystagmus. A, Hematoxylin-eosin–stained cross section obtained from the medial rectus muscle of a patient with infantile nystagmus (patient 10). Arrows indicate myofibers with central nucleation. Bar is 20 μ m. B, Quantification of the percentage of myofibers with central nucleation in normal rectus muscles compared with muscles from patients with infantile nystagmus. The 2 muscles obtained from the 7-year-old control are depicted separately to demonstrate their similarity with data from the adult control muscles; however, for statistical analysis, all the control muscles were pooled. * P .05. Error bars indicate SE.

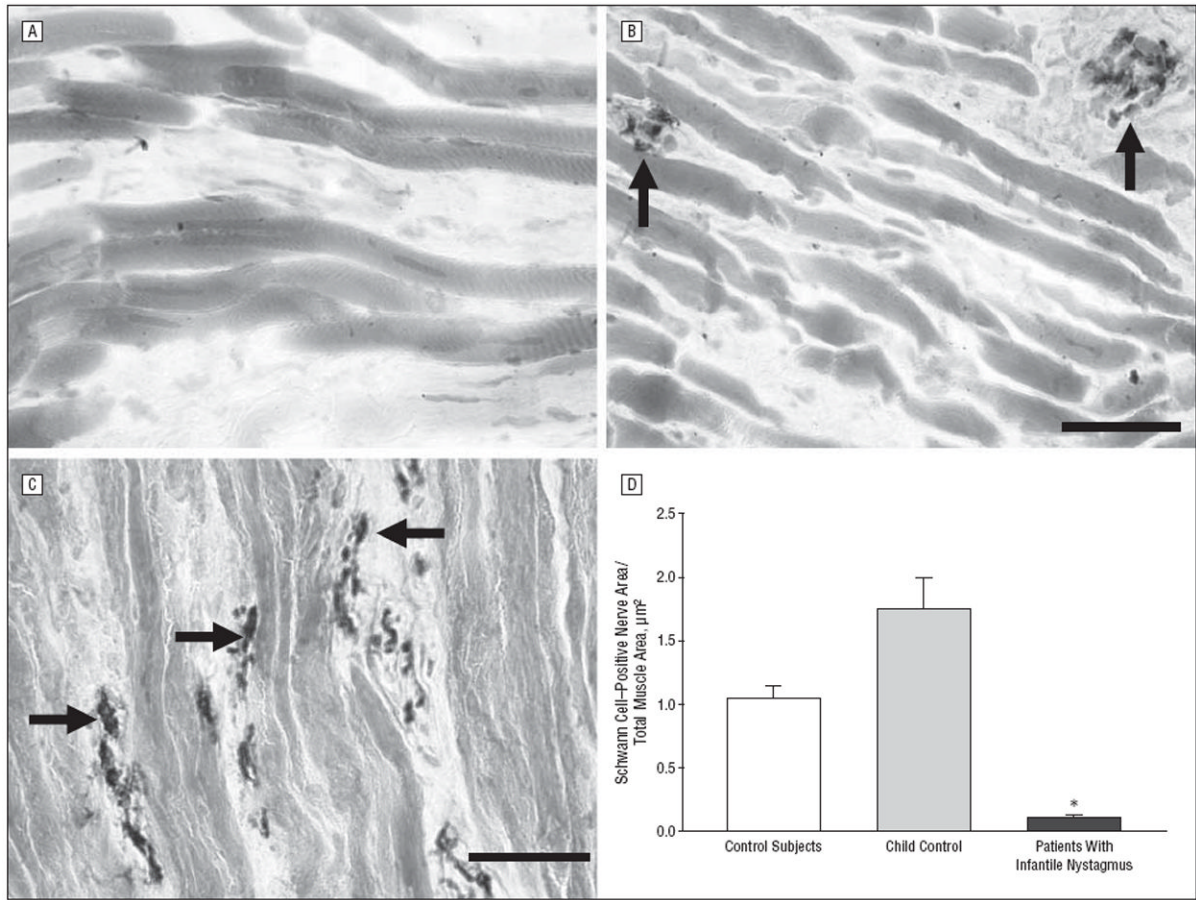


Figure 5.

Sections from controls, patients with infantile nystagmus, and a patient with vertical strabismus that have been immunostained for the presence of Schwann cell myelin. A, Typical appearance of muscle from a patient with infantile nystagmus showing extremely sparse innervation (n=10). B, Typical appearance of myelinated nerve fiber content in control extraocular muscles (n=10). C, Typical appearance of myelinated nerves from a patient with vertical strabismus (n=1). Bars are 20 μm . D, Quantification of mean Schwann cell area per total muscle area from controls (n=10), a child control (n=1), and patients with infantile nystagmus (n=10). The 2 muscles obtained from the 7-year-old control are depicted separately to demonstrate their similarity with data from the adult control muscles; however, for statistical analysis, all the control muscles were pooled. * P .05. Arrows indicate Schwann cell-positive nerve bundles; error bars, SE.

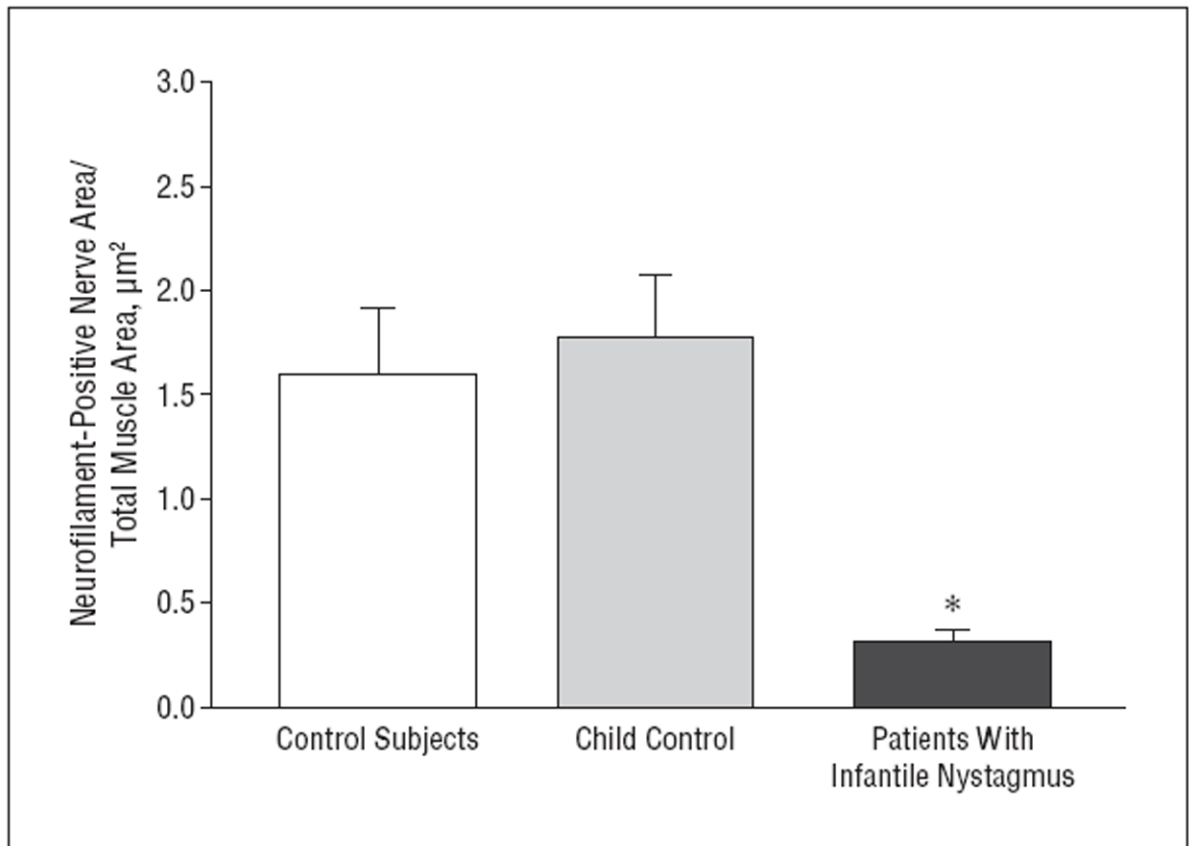


Figure 6.

Quantification of mean nerve fiber area per total muscle area from controls (n=10) and patients with infantile nystagmus (n=10). The 2 muscles obtained from the 7-year-old control are depicted separately to demonstrate their similarity with data from the adult control muscles; however, for statistical analysis, all the control muscles were pooled. * $P < .05$. Error bars represent SE.

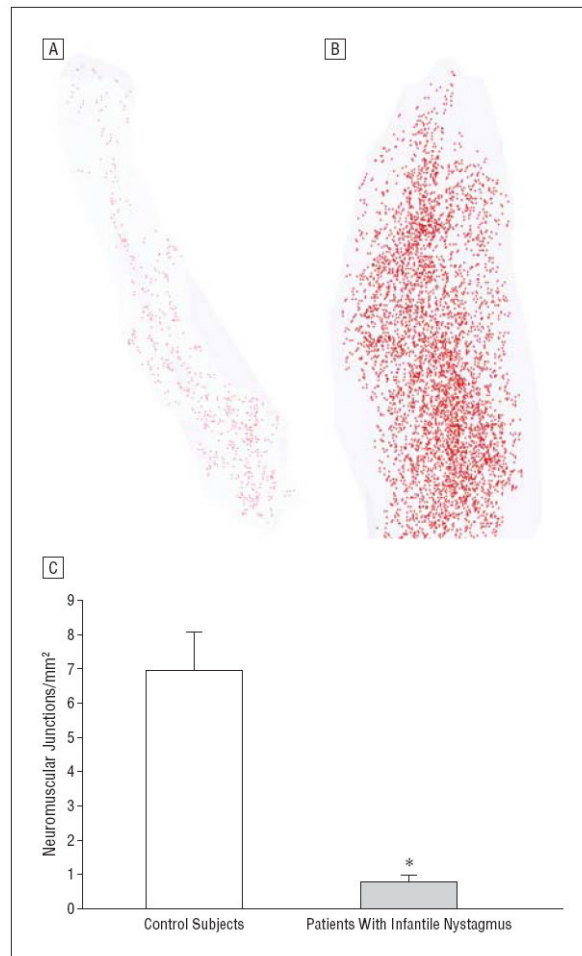


Figure 7. Immunostaining for visualization of neuromuscular junctions. Three-dimensional reconstructions of the neuromuscular junctions from the rectus muscles of a patient with infantile nystagmus (A) and a control monkey (B), with the monkey muscle having the same length as the human muscle selected. Each red dot represents 1 neuromuscular junction. Every 10th section was analyzed morphometrically. C, Quantification of the density of neuromuscular junctions from rectus muscles from controls (n=10) and patients with infantile nystagmus (n=10). * P .05. Error bars represent SE.

Table

Characteristics of 10 Patients With Infantile Nystagmus Without Associated Conditions

Patient No./Sex/Age at Surgery, y	Nystagmus Diagnosis ^a	Muscles Harvested
1/F/4½	Horizontal pendular	RLR, LMR
2/F/7	Left-beating jerk	LLR, RMR
3/M/5	Right-beating jerk	RLR, LMR
4/M/52	Left-beating jerk with chin-up head posture	RSR, LSR
5/F/6	Horizontal	LMR, RLR
6/F/6	Horizontal jerk with head turn	LLR, RMR
7/F/5	Horizontal jerk	RLR, LMR
8/F/12	Horizontal jerk with head posture	LLR, RMR
9/M/6	Left beating	LLR, RMR
10/F/7	Right beating	RLR, LMR

Abbreviations: LLR, left lateral rectus; LMR, left medial rectus; RLR, right lateral rectus; RMR, right medial rectus.

^aNo patients had diagnosed associated sensory afferent defects.